

DETC2003/VIB-48455

A MODEL FOR THE COUPLED LIFT AND DRAG ON A CIRCULAR CYLINDER

Ali H. Nayfeh*

Department of Engineering Science and Mechanics, MC 0219
Virginia Polytechnic Institute and State University
Blacksburg, Virginia 24061-0219
Tel: 540-231-5453, Fax: 540-231-2290
Email: anayfeh@vt.edu

Farouk Owis

Department of Aerospace Engineering
Cairo University
Cairo, Egypt

Muhammad R. Hajj

Department of Engineering Science and Mechanics, MC 0219
Virginia Polytechnic Institute and State University
Blacksburg, Virginia 24061-0219
Tel: 540-231-4190, Fax: 540-231-4574
Email: mhajj@vt.edu

ABSTRACT

The time-varying coupled lift and drag coefficients acting on a circular cylinder are modeled. Data used for the model are obtained by numerically solving the unsteady Reynolds-Averaged Navier Stokes equations over a wide range of Reynolds numbers. Using spectral moments, we determine the frequency components in the lift and drag coefficients and their phase relations. Using a perturbation technique, we obtain approximate solutions of both the van der Pol and Rayleigh equations. By fitting the amplitude and phase relations, we find that the van der Pol equation is the suitable model for the lift. The Rayleigh equation fails to give the correct phase relation. Because the major frequency in the drag component is twice that of the lift, the drag component is modeled as a quadratic function of the lift. Through analysis with higher-order spectral moments, the correct quadratic relation of the lift that yields the drag is determined. The model and results presented here are a first step in the development of a reduced-order model for vortex-induced vibrations, which includes the motions of the cylinder.

INTRODUCTION

Modeling of vortex-induced vibrations of circular cylinders is of particular interest in oil production-riser systems used in offshore platforms. These vibrations involve complicated interactions between the cylinder motions and the fluid forces, including the relation between the drag and lift forces, which involve nonlinear couplings that have their sources in the dependence of the pressure on the complex flow field. Additionally, because the cylinder's motions affect the fluid forces and because these forces affect the cylinder's motions, resonance phenomena between the forces and the motions must be considered. An ultimate solution for this problem would be a time-domain numerical simulation of the fluid flow and the cylinder's response, including elastic effects. In this solution, the fluid and the cylinder would be treated as a single dynamical system and all of the governing equations would be solved simultaneously and interactively in the time domain. Obviously, this is a formidable task, especially when considering the fact that the Reynolds numbers associated with full-scale flows in oil production-riser systems are quite large. Alternatively, one could construct a model that takes into consideration all of the physical aspects and is capable

*Address all correspondence to this author.

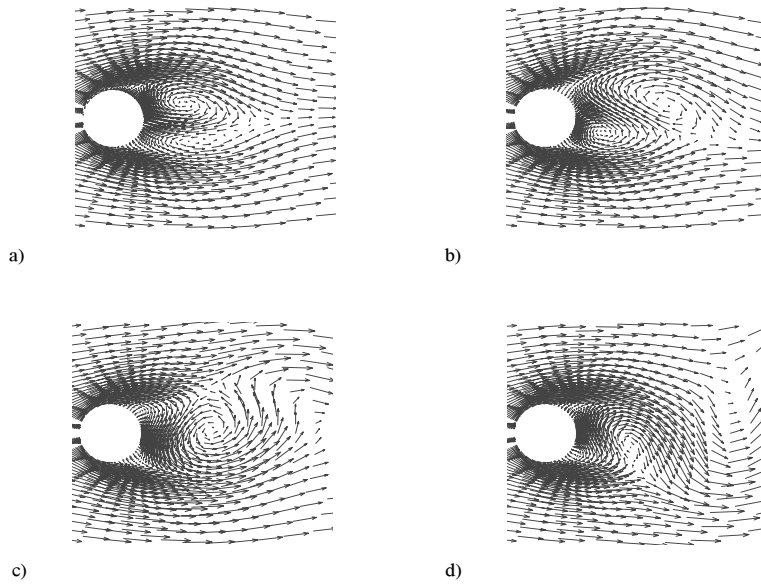


Figure 1. Time snaps of the velocity vectors in the flow field, $Re = 100000$

of predicting vortex-induced vibrations. The long-term objective for this work is to develop such a model by successive tasks that build on models for the time variations of the fluid forces, cylinder response, and their interactions. In this paper, we model the time-varying coupled lift and drag forces, which act on a stationary circular cylinder over a wide range of Reynolds numbers.

A well-known model for the lift force acting on a circular cylinder when subjected to a fluid flow is the lift wake oscillator proposed by Hartlen and Currie [1]. In this model, the lift is represented by a Rayleigh equation. Currie and Turnball [2] proposed a similar model for the fluctuations of the drag coefficient. To study resonant responses of suspended elastic cables, Kim and Perkins [3] used a coupled model, based on two van der Pol equations for the drag and lift coefficients. In this model, the drag is affected by many possibilities of quadratic couplings of the lift. Additionally, the lift is affected by its quadratic coupling with the drag. These couplings were introduced based on the fact that the main frequency of the drag component is twice the main frequency of the lift component. The objective of this work is to develop a model for the time-varying drag and lift coefficients acting on a stationary circular cylinder using solutions of the Navier Stokes equations over a wide range of Reynolds numbers. Using perturbation analysis, higher-order spectral moments, and the time series of the lift coefficient obtained from numerical solutions of the Navier-Stokes equations, we identified the coefficients in the governing equation for the lift. Again, using phase relations obtained from higher-order spectral moments, we related the drag component to the lift. The model presented here is a first step in the development of a reduced-order

model for vortex-induced vibrations that includes the cylinder's motions as discussed above.

NUMERICAL SIMULATION OF FLOW FIELD

The drag and lift forces acting on the cylinder are determined by integrating the surface pressures. These pressures are obtained from a numerical solution of the unsteady Reynolds averaged Navier-Stokes equations. The artificial compressibility method is used to couple the continuity and momentum equations. For turbulence closure, the two-equation $k - \omega$ model is used. Because of its sensitivity to free-stream conditions, the model switches from the $k - \omega$ model near the wall to the $k - \epsilon$ model away from the wall. The equations are solved on a structured grid using a second-order finite-difference scheme. The convective terms are discretized using a second-order upwind-difference scheme. The physical-time terms, which represent flow unsteadiness, are switched to the right-hand side and used as source terms. These terms are discretized using a second-order three-point backward difference formula. Different boundary conditions are used in the simulations, including inflow, outflow, and no-slip. All of the boundary conditions are treated implicitly in the code to reduce the restriction on the time step and to increase its stability. For the inflow boundary, the velocity components are specified, while the pressure is extrapolated from the interior points. At the outflow boundary, the pressure is specified, whereas the velocity components are extrapolated from the computational domain. On the cylinder surface, the velocities are set equal to the cylinder velocity. In addition, similar boundary conditions are set for the turbulence quantities.

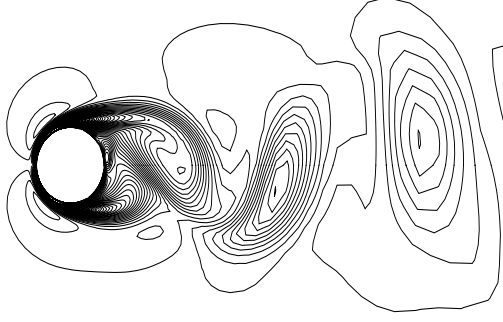


Figure 2. A snap shot of the vorticity contours in the flow field, $Re = 100000$

Time variations in the flow field around the circular cylinder are shown in Fig 1. The results clearly show how the vorticity is generated at the separation points over the cylinder with vortices forming in the wake of the cylinder, Fig 1a. As shown in Fig 1b, the vorticity generated at the bottom side of the cylinder moves up and cuts the upper vorticity to yield vortex shedding of the upper vortex. This phenomenon is reversed and repeated as shown in Fig 1c and Fig 1d, respectively. This reverse in the vorticity yields time variations in the surface pressures over the cylinder and is the cause for the periodic variations in the lift and drag coefficients. Figure 2 shows the vortex shedding with vortices forming in the near wake and diffusing further downstream.

LIFT AND DRAG MODELING

Figures 3 and 4 show the spectra of the lift and drag coefficients at two representative Reynolds numbers, namely 20000, and 100000, respectively. At $Re = 20000$, the spectrum of the lift coefficient shows a major peak at the shedding frequency $f = 0.237$. At $Re = 100000$, the peak is at 0.254. A frequency component at the third harmonic $3f$ is also present in the spectra of the lift coefficient in Fig 3 and Fig 4, a. It is three to four orders of magnitude smaller than the major peak at f .

The presence of peaks corresponding to the shedding frequency and its third harmonic suggests that the lift coefficient on the circular cylinder can be modeled by either the Rayleigh

equation or the van der Pol equation. The Rayleigh equation is

$$\ddot{l} + \omega_s^2 l - \mu_r \dot{l} + \alpha_r l^3 = 0 \quad (1)$$

and the van der Pol equation is

$$\ddot{l} + \omega_s^2 l - \mu_v \dot{l} + \alpha_v l^2 \dot{l} = 0 \quad (2)$$

In these equations, ω_s is the shedding frequency, μ and α represent the linear and nonlinear damping coefficients, and the subscripts r and v are used to denote these coefficients in the Rayleigh and van der Pol equations, respectively. The parameters μ and α are positive so that the linear damping is negative and the nonlinear damping is positive. As a result, small motions grow and large motions decay resulting in stable limit cycles. It is of interest to note also that the van der Pol equation can be obtained by differentiating the Rayleigh equation and performing a derivative substitution.

Using the method of multiple scales [4; 5], we obtain the following approximate solution for equation (1):

$$l = a \cos(\omega_s t + \beta) + \frac{\alpha_r \omega_s}{32} a^3 \cos(3\omega_s t + 3\beta - \frac{1}{2}\pi) \quad (3)$$

where β is a constant phase and

$$\dot{a} = \frac{1}{2} \mu_r a - \frac{3\omega_s^2 \alpha_r}{8} a^3 \quad (4)$$

Using separation of variables, we find that the solution of equation (4) is given by

$$a^2 = \frac{4\mu_r}{3\omega_s^2 \alpha_r - e^{-4\mu_r(t+c)}} \quad (5)$$

As $t \rightarrow \infty$, it follows from equation (5) that

$$a \rightarrow \frac{2}{\omega_s} \sqrt{\frac{\mu_r}{3\alpha_r}} \quad (6)$$

Similarly, using the method of multiple scales [4; 5], we obtain the following approximate solution for equation (2):

$$l = a \cos(\omega_s t + \beta) + \frac{\alpha_v}{32\omega_s} a^3 \cos(3\omega_s t + 3\beta + \frac{1}{2}\pi) \quad (7)$$

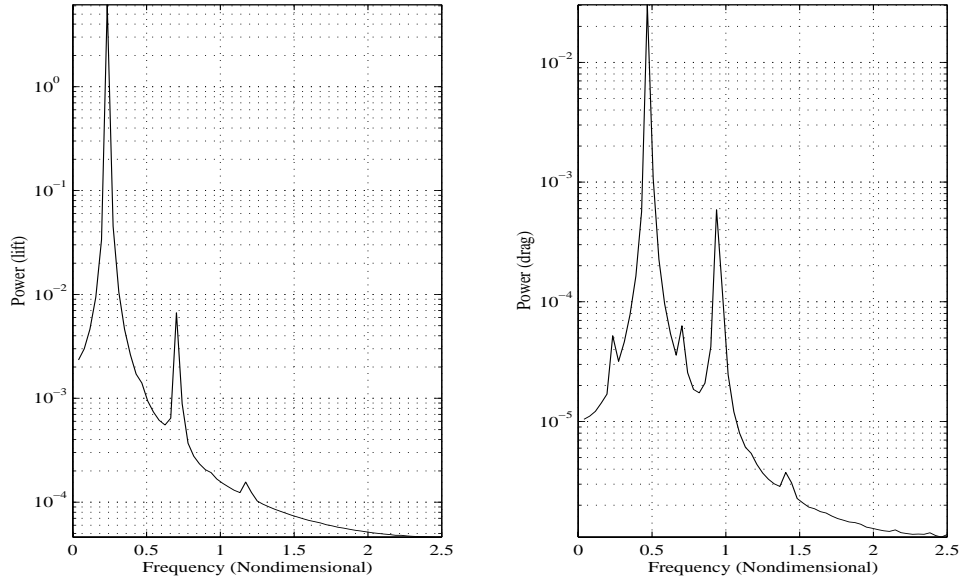


Figure 3. Lift and drag spectra at Re=20000

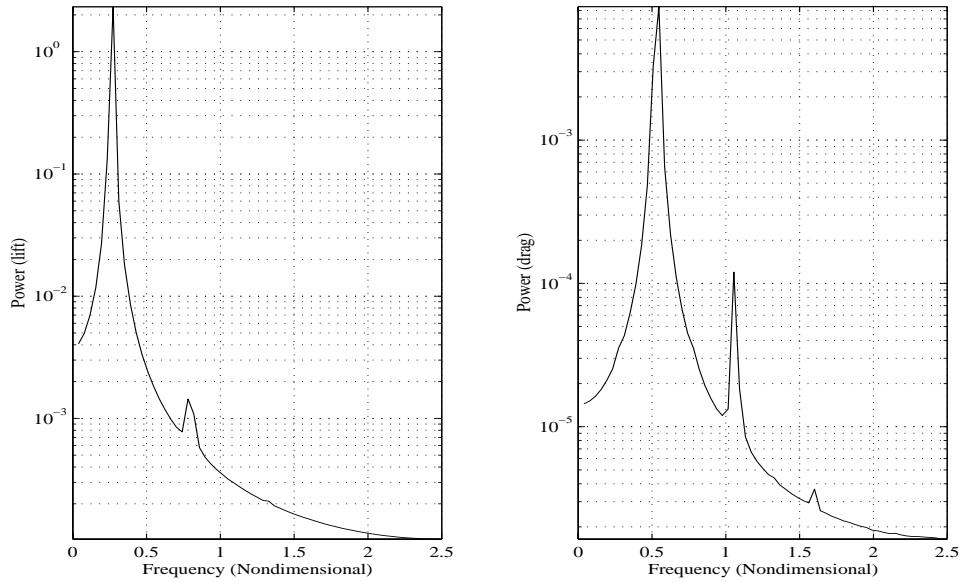


Figure 4. Lift and drag spectra at Re=100000

where β is a constant phase and

$$\dot{a} = \frac{1}{2}\mu_v a - \frac{\alpha_v}{8}a^3 \quad (8)$$

Using separation of variables, we find that the solution of equa-

tion (8) is given by

$$a^2 = \frac{4\mu_v}{\alpha_v - e^{-4\mu_v(t+c)}} \quad (9)$$

As $t \rightarrow \infty$, it follows from equation (9) that

$$a \rightarrow 2\sqrt{\frac{\mu_v}{\alpha_v}} \quad (10)$$

It is of interest to note that equations (3) and (7) show a difference in the phase of the third harmonic in relation to the phase of the vortex shedding frequency. Determining this phase will yield the correct modeling equation for the lift coefficient. In order to do so, and based on the lift spectra of Fig 3 and Fig 4, we represent the lift as

$$l = a_1 \cos(\omega_s t) + a_3 \cos(3\omega_s t + \gamma) \quad (11)$$

where ω_s is the shedding frequency, a_1 is the amplitude of the component at ω_s , a_3 is the amplitude at $3\omega_s$, and γ represents the phase of the third harmonic when the phase of the fundamental component is zero. Comparing equation (11) with equations (3) and (7), we conclude that the lift can be modeled by either the Rayleigh or van der Pol equation depending on whether $\gamma \approx -\frac{1}{2}\pi$ or $\gamma \approx \frac{1}{2}\pi$. Consequently, to match the time series predicted with the van der Pol or Rayleigh equation with that obtained from the numerical simulation, one needs to determine accurately the amplitudes a_1 and a_3 as well as the phase γ . Because the phase γ is defined as the phase of the third harmonic when the phase of the vortex shedding frequency is zero, it can be recovered, at any time, by the phase relation [6]

$$\gamma = \phi(3\omega_s) - 3\phi(\omega_s) \quad (12)$$

where $\phi(\omega_s)$ and $\phi(3\omega_s)$ are, respectively, the phases of the spectral components at the vortex shedding frequency and its third harmonic. This relation can be measured as the phase of the auto-trispectrum between these two components, which is defined as

$$S_{lll} = \langle L(3f)L^*(f)L^*(f)L^*(f) \rangle \quad (13)$$

where $L(f)$ is the Fourier Transform of the lift time series $l(t)$, the asterisk represents the complex conjugate, and $\langle \dots \rangle$ denotes ensemble averaging. Thus, the Fourier Transform of the time series derived from the numerical simulation yields the amplitudes of the peaks at the vortex shedding frequency and its third harmonic as well as their phase relation.

As for the drag coefficient, the spectra in Fig 3 and Fig 4 show that, in each case, the drag has two peaks at the second and fourth harmonics of the vortex shedding frequency. Because the drag and lift are the result of the pressure distribution on the surface of the cylinder, it is feasible to relate the drag to the lift directly. The fact that the major component in the spectrum of the drag coefficient is at twice the shedding frequency suggests that the drag is a quadratic function of the lift; that is, the drag is proportional to either l^2 , \dot{l}^2 or $l\dot{l}$. Of these three forms, the

correct form must yield the right phase relation between the drag and lift. Because the frequency of the major component of the drag is twice the frequency of the major component in the lift, this phase relation is given by $\phi(2\omega_s)$ in the drag time series - $2\phi(\omega_s)$ in the lift time series. As shown in [6], this phase can be measured as the phase of the cross bispectrum between $2f$ in the drag and f in the lift, which is defined as

$$S_{dll} = \langle D(2f)L^*(f)L^*(f) \rangle \quad (14)$$

where $D(f)$ is the Fourier Transform of the drag time series $d(t)$.

RESULTS AND DISCUSSION

The time series for the lift and drag coefficients obtained from the numerical solutions were analysed to determine the parameters discussed above. It is important to note that the sampling frequency and record length had to be adjusted between the different runs in order to accurately predict the amplitudes of the main frequencies and the phase relations discussed above. For the lift time series, the phase of S_{lll} was approximately $\frac{1}{2}\pi$ for all runs and hence the van der Pol equation should be used to model the lift. By comparing equation (11) with equations (7) and (10), we find that

$$\alpha_v = \frac{32\omega_s a_3}{a_1^3} \quad (15)$$

and

$$\mu_v = \frac{1}{4}\alpha_v a_1^2 \quad (16)$$

These equations are then used to determine the linear and nonlinear damping coefficients in the van der Pol equation from the amplitudes of the Fourier components in the time series. Variations of f , a_1 , and a_3 with the Reynolds number are shown in Table 1. It should be noted here that the nondimensional vortex shedding frequency or Strouhal number is in agreement with experimental results for the Reynolds number 200. At higher Reynolds numbers, the Strouhal numbers are overestimated. This is most likely due to the increased three-dimensional effects [7].

Reynolds#	f	a_1	a_3
200	0.193	0.6184	0.0044
1000	0.2295	1.205	0.039
2000	0.2368	1.394	0.052
10000	0.2391	1.793	0.049
20000	0.2368	1.728	0.055
40000	0.2510	1.465	0.040
100000	0.2538	1.056	0.021
1000000	0.2550	1.321	0.033

The drag consists of two components. The first is a mean component that is independent of the lift and the second is a periodic component that is related to the unsteady lift. Because the phase relation between the drag component and the lift as defined above is near $3\pi/2$ in all records, the periodic component of the drag must be proportional to $-\dot{l}$. Consequently, the drag coefficient can be modeled by

$$d = d_m - \frac{k_1}{a_1^2 \omega_s} \dot{l} \quad (17)$$

Variations of the mean drag d_m with the Reynolds number, obtained independently as a mean value from the time series of the drag, and of the coefficient k_1 , which is the amplitude of the major frequency component in the drag, are shown in Table 2.

Reynolds#	d_m	k_1
200	1.18	0.0368
1000	1.29	0.135
2000	1.36	0.175
10000	1.62	0.129
20000	1.48	0.112
40000	1.32	0.0786
100000	0.85	0.0636
1000000	1.06	0.0773

The parameters in Tables 1 and 2 were used to estimate μ_v , α_v , and $k_1/a_1^2 \omega_s$. These values were then used in conjunction with equations (2) and (17) to predict the steady-state lift and drag. A comparison of the simulated and modeled lift and drag coefficients at $Re = 200, 20000$ and 100000 is shown in Figs 5-10. Obviously, the results show excellent agreement across the entire range of Reynolds numbers considered.

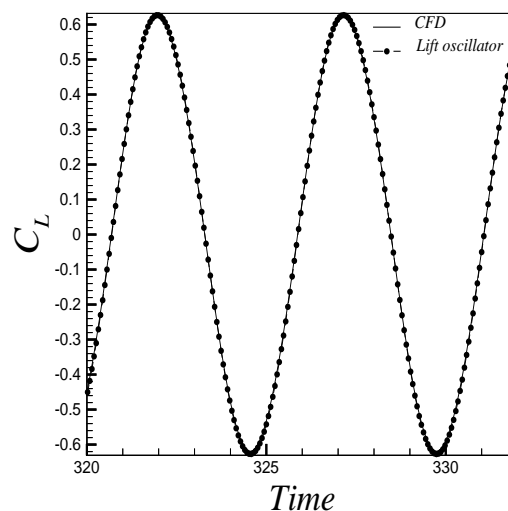


Figure 5. Comparison of simulated and modeled lift coefficient, $Re = 200$

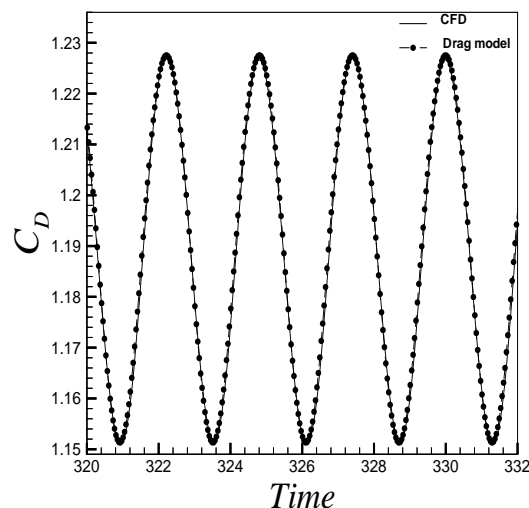


Figure 6. Comparison of simulated and modeled drag coefficient, $Re = 200$

CONCLUSIONS

In this work, the time-varying coupled lift and drag coefficients acting on a circular cylinder are modeled. Numerical solutions of the unsteady Reynolds-Averaged Navier Stokes equations were obtained to generate a database for the model. Spectral analysis of the time series of the lift coefficient showed that it contained a major component at the vortex shedding frequency

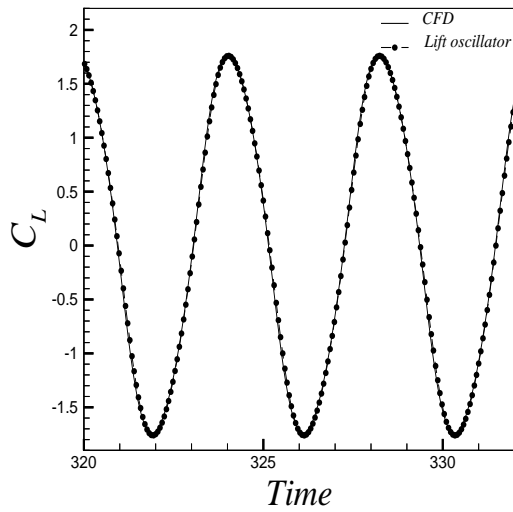


Figure 7. Comparison of simulated and modeled lift coefficient, $Re = 20000$

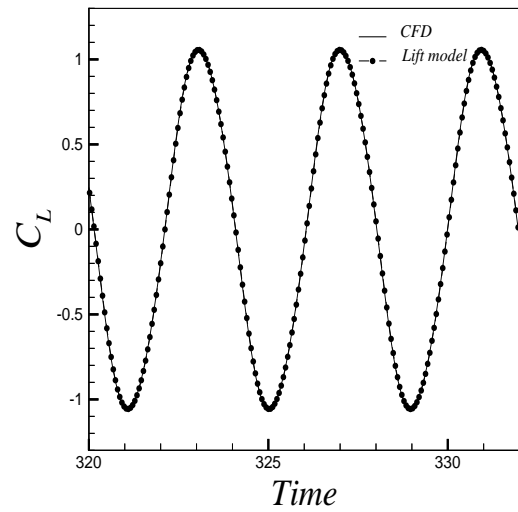


Figure 9. Comparison of simulated and modeled lift coefficient, $Re = 100000$

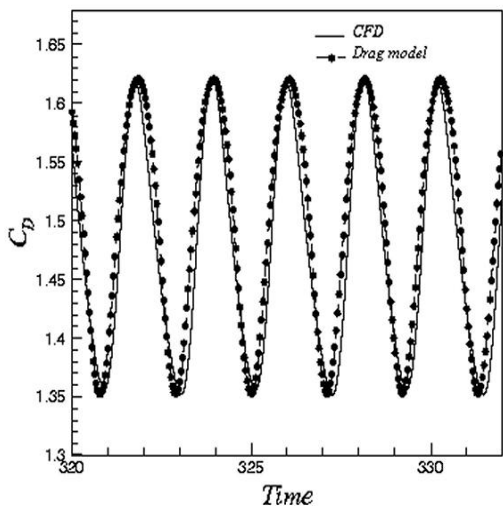


Figure 8. Comparison of simulated and modeled drag coefficient, $Re = 20000$

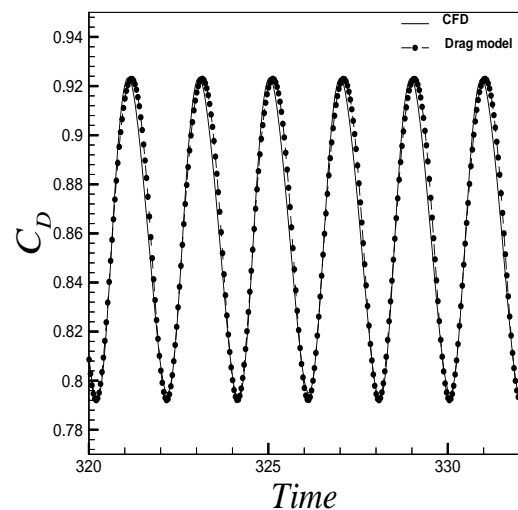


Figure 10. Comparison of simulated and modeled drag coefficient, $Re = 100000$

and a smaller one at its third harmonic, implying that the lift component can be modeled using either the Rayleigh or van der Pol equation. Approximate solutions of both equations showed that only one of these equations can be used to model the lift. This is dependent on the phase relation between the frequencies of the two components. Measurement of this phase relation with the auto-trispectrum showed that the lift can be modeled only by

the van der Pol equation. Frequency domain analysis of the drag showed that it contained the second and fourth harmonics of the vortex shedding frequency, implying that the drag is a quadratic function of the lift. Using the phase of the cross-bispectrum between the drag and lift time series, we determined that the unsteady component of the drag must be proportional to $-l^2$ where l is the lift coefficient. The models and results presented here

are a first step in the development of a reduced-order model for vortex-induced vibrations that includes the cylinder's motions.

REFERENCES

- [1] Hartlen, R. T., and Currie, I. G., 1970, "Lift-Oscillator Model of Vortex-Induced Vibrations", *Journal of Engineering Mechanics*, Vol. 96(5), pp. 577-591.
- [2] Currie, I. G., and Turnbull, D. H., 1987, "Streamwise Oscillations of Cylinders Near the Critical Reynolds Number" *Journal of Fluids and Structures*, Vol. 1, pp. 185-196.
- [3] Kim, W. J., and Perkins, N. C., 2002, "Two-Dimensional Vortex-Induced Vibrations of Cable Suspensions", *Journal of Fluids and Structures*, Vol. 16(2), pp. 229-245.
- [4] Nayfeh, A. H., 1973, *Perturbation Methods*, Wiley, New York.
- [5] Nayfeh, A. H., 1981, *Introduction to Perturbation Techniques*, Wiley, New York.
- [6] Hajj, M. R., Miksad, R. W., and Powers, E. J., 1993, "Fundamental-Subharmonic Interaction: Effect of Phase Relation", *Journal of Fluid Mechanics*, Vol. 256, pp. 403-426.
- [7] Mittal, R., and Balachandar, S., 1995, "Effect of Three-Dimensionality on the Lift and Drag of Nominally Two-Dimensional Cylinders" *Physics of Fluids*, Vol. 7(8), pp. 1841-1865.